



*Original Research Article*

*Original Research Article*

## **Hydrological Functioning of a Bromeliad Green Roof: Interception Capacity and Evapotranspiration**

**Bernard Busch<sup>1</sup>, Mohammad K. Najjar<sup>2</sup>, Victoria O. Souza<sup>1</sup>, Elaine G. Vazquez<sup>\*3</sup>**

<sup>1</sup> Departamento de Construção Civil, Universidade Federal do Rio de Janeiro, Brazil, e-mail: [bernardbusch@poli.ufrj.br](mailto:bernardbusch@poli.ufrj.br); [victoria@mecanica.coppe.ufrj.br](mailto:victoria@mecanica.coppe.ufrj.br)

<sup>2</sup> Programa de Engenharia Ambiental, Universidade Federal do Rio de Janeiro, Brazil  
e-mail: [mnajjar@poli.ufrj.br](mailto:mnajjar@poli.ufrj.br)

<sup>3</sup> Programa de Engenharia Urbana Universidade Federal do Rio de Janeiro, Brazil  
e-mail: [elaine@poli.ufrj.br](mailto:elaine@poli.ufrj.br)

Cite as: França Busch, B., K. Najjar, M., O. Souza, V., Vazquez, E., Hydrological Functioning of a Bromeliad Green Roof: Interception Capacity and Evapotranspiration, *J.sustain. dev. energy water environ. syst.*, 14(4), 1140745, 2026, DOI: <https://doi.org/10.13044/j.sdewes.d14.0745>

### **ABSTRACT**

This work presents an analysis on the contribution of plant interception and evapotranspiration on a green roof composed of bromeliads based on experimental tests carried out in a prototype. The objective is to calculate the volume of water intercepted by bromeliads and the volume of water that undergoes evapotranspiration and compare with the volume precipitated over the green roof and with the volume retained to better understand the mechanism of interaction between the parts. The main purpose is to improve the efficiency as a compensatory technique in urban drainage, which aids in minimizing urban flooding by all major cities. A literature review was made on the hydrological cycle and its stages and a description of the history and advantages of green roofs, aiming at a better understanding of the operation of the system. This work contributes to improving the efficiency of green roofs with regard to rainwater retention.

### **KEYWORDS**

*Green roof; Interception; Evapotranspiration; Hydrological cycle; Urban drainage*

### **INTRODUCTION**

Human activities and industries, whether concentrated in urban centers or dispersed across rural areas, have significantly altered the environment [1]. In this context, the environment is defined as the set of physical and chemical elements, together with natural and social ecosystems, within which human beings are embedded both individually and collectively [2]. These interactions occur through dynamic processes that seek to reconcile the development of human activities with the preservation of natural resources and the maintenance of essential environmental characteristics, in compliance with established environmental quality standards [3].

\* Corresponding author

However, when such interactions exceed the adaptive capacity of natural systems, they generate localized disturbances and trigger nonlinear responses and threshold effects, leading abrupt changes in ecosystem structure and function. These thresholds, often referred to as tipping points, mark critical transitions beyond which recovery becomes difficult or even impossible without significant external intervention. As a result, environmental impacts propagate across spatial and temporal scales, ultimately contributing to global environmental change [4]. This cross-scale propagation is reinforced by feedback mechanisms that couple human and natural systems [5]. For instance, land-use change such as deforestation alters surface albedo, evapotranspiration, and carbon storage, which in turn influence atmospheric circulation and climate patterns [6]. These climatic shifts can further intensify land degradation, biodiversity loss, and water scarcity, creating reinforcing loops that amplify the initial disturbance [7]. In this sense, global environmental change emerges as a collection of isolated processes and as a network of interdependent dynamics, where changes in one subsystem cascade into others [8]. Acting cumulatively and systemically, global environmental change affects the Earth as an integrated system. Processes such as climate change; alterations in atmospheric chemistry and biogeochemical cycles; changes in land use and land cover; global chemical pollution; and disruptions of the hydrological cycle exert widespread impacts on the global ecosystem, effects that are already observable even in the most remote regions of the planet [9].

Agricultural practices, livestock production, economic development, and urban expansion directly alter natural systems by modifying key biological and geographical attributes, including vegetation cover, fauna, soil permeability, surface absorptivity, and albedo [10]. These activities also influence local and regional climatic conditions, as well as the physical and chemical properties of atmospheric air, soils, and water resources, affecting processes such as surface runoff, river dynamics, and groundwater recharge. Among the environmental challenges associated with these anthropogenic pressures, those most pronounced in urban environments include the reduction of green spaces driven by civil construction and widespread soil sealing, which disrupts the natural functioning of the hydrological cycle and contributes to a range of urban environmental problems [11].

Anthropogenic pressures and urbanization substantially affect urban hydrological processes, particularly the circulation and distribution of water. The removal of vegetated areas and the widespread sealing of natural surfaces significantly reduce key components of the hydrological cycle (namely interception, evaporation, transpiration, and infiltration) relative to total precipitation. These processes play a critical role in retaining rainfall and attenuating surface runoff, thereby contributing to the mitigation of both the frequency and magnitude of floods and inundation events [12]. As these regulating mechanisms are progressively weakened in urban environments, storm water management has emerged as an urgent challenge for cities. The increasing dominance of impervious surfaces, such as roads and buildings, limits rainfall retention and leads to higher volumes and velocities of surface runoff. In response to this imbalance, the incorporation of green infrastructure has gained prominence as a strategy to offset excessive urban densification and soil sealing [13]. According to Rola et al. [14], green areas and nature-based interventions aim to transform buildings and urban spaces into functional biotopes in an economically and ecologically optimized manner, which, when interconnected through green corridors, enhance atmospheric circulation and improve urban microclimatic conditions.

By recovering the principles of greening built-up areas and aligning with the guidelines of Agenda 21, it seeks to mitigate the impacts caused by urban development, scientifically

addressing environmental demands and redirecting cities toward sustainable development, thereby achieving greater integration between the urban space, citizens, and nature.

According to Mora-Melià [15], green roofs constitute an effective strategy for urban flood mitigation by promoting the temporary retention and delayed release of rainfall. This function is achieved through their role as compensatory techniques in urban drainage systems, whereby precipitation volumes are attenuated by vegetated covers that enable surface storage, water uptake by vegetation, and retention within the substrate. Green roofs reduce surface runoff and consequently decrease the volume of water conveyed to urban drainage networks by retaining a portion of incident rainfall [16], [17]. In addition to storm water regulation, the retained water may be treated and reused for non-potable purposes, such as toilet flushing, surface cleaning, and landscape irrigation, thereby improving urban water efficiency and alleviating pressure on conventional water supply systems [18].

Consequently, this mechanism can influence the hydrological balance of the catchment by acting as a temporary storage system that retains part of the incoming precipitation. This storage occurs both on vegetative surfaces (interception) and within the substrate layer, where water is held before being gradually released through drainage or returned to the atmosphere via evapotranspiration [19]. As a result, interception tends to attenuate seasonal flow variability, delaying runoff responses and reducing flood peak magnitudes [20]. This temporal redistribution is particularly relevant in urban environments, where impervious surfaces typically generate rapid runoff and exacerbate peak discharges [21]. Within the context of green roofs, there was a need to explore some aspects, such as the influence of plant interception and evapotranspiration, in order to better understand its benefits as a compensatory urban drainage technique.

It is known that at the event scale, evaporation losses of rainfall intercepted by canopy are a few millimetres, which is often not much in comparison to other stocks in the water balance [22]. Nevertheless, at yearly scale, the number of times that the canopy is filled by rainfall and then depleted can be so large that the interception flux may become an important fraction of rainfall [23]. These processes become even more complex due to the interaction between vegetation characteristics, substrate properties, and climatic conditions. Plant interception capacity varies with leaf area index, canopy structure, and rainfall intensity [24], while evapotranspiration rates depend on solar radiation, wind speed, air temperature, and soil moisture availability [25]. These factors control the antecedent moisture condition of the system, which is a key determinant of its retention capacity during subsequent rainfall events. Therefore, green roofs behave as dynamic hydrological components whose performance evolves over time [26]. For this reason, there is a clear need to further investigate the relative contributions of plant interception and evapotranspiration in green roof systems, particularly under different seasonal and climatic scenarios. A better understanding of these processes can improve the parameterization of hydrological models and support the design of more efficient green roof configurations. Ultimately, such insights reinforce the role of green roofs as a compensatory urban drainage technique, capable not only of reducing runoff volumes but also of mitigating peak flows and enhancing the resilience of urban water management systems.

Flooding and inundation are considered as complex urban phenomena with cascading impacts across infrastructure, public health, and socio-economic systems [27]. They disrupt urban mobility, causing traffic chaos and rendering some inaccessible areas, where floods can paralyze entire transport networks, including public transit systems, emergency response routes, and supply chains [28]. They lead to financial economic consequences such as damage

to vehicles and residences. Flood events can interrupt commercial activities, reduce workforce productivity, and impose significant recovery costs on both households and municipalities [29]. Besides, they pose risks to the population, as many people are injured when attempting to walk through flooded streets, which also contributes to the transmission of waterborne diseases [30]. Another serious problem caused by flooding is slope failure and landslides, which represent a high risk of structural collapse and burial of dwellings, leaving many people homeless and, depending on the severity of the events, potentially resulting in fatalities [31].

With the aim of restoring environmental balance and mitigating the problems affecting the hydrological cycle, the use of green roofs has emerged as a viable solution. In addition to their ability to retain storm water and thus reduce peak runoff directed to storm water drainage systems, green roofs provide several other benefits, such as mitigation of urban heat islands, acoustic insulation, increased biodiversity, and improved air quality.

Within the context of green roofs, there is a need to further investigate certain aspects, particularly the influence of vegetation interception and evapotranspiration, in order to better understand their effectiveness as a compensatory urban drainage technique.

Climatic conditions and differences in green roof configuration, i.e., substrate type and depth, as well as plant species selection, drive this variation in performance [32]. Evapotranspiration is influenced by substrate characteristics, depth and species selection [25], [33], [34].

Vegetation interception is a key variable controlling hydrological and geo-environmental processes, such as erosion, landslides, and floods, and is essential for modeling infiltration, percolation, and runoff [35]. However, field measurements are time-consuming and subject to high variability, making rainfall simulators a reliable alternative [36]. Mendes et al. [37] applied this approach to *Paspalum notatum* (bahiagrass) and a tropical soil, obtaining an average interception of 5.1 mm under a 15° slope, rainfall intensity of 86 mm h<sup>-1</sup>, and duration of 60 minutes.

Similarly, rainfall interception has also been investigated at the urban scale. At the COSMO experimental site, located in the northern Kanto Plain, Japan (39°04'N, 139°07'E), interception was analyzed from the perspective of water and energy balance under a temperate climate with a rainy season in June–July and a dry winter. According to Nakayoshi et al. [38], interception was estimated as the residual between measured rainfall and runoff over a five-month period, with an average value of 6% of gross rainfall, which is lower than typical values observed in forests.

The objective of this study is to analyze the interception of vegetation and evapotranspiration, through experimental tests carried out in the prototype of green roof located in the Experimental center of Environmental Sanitation (CESA) of the Federal University of Rio de Janeiro – Universidade Federal do Rio de Janeiro (UFRJ). Considering the wide range of variables involved, this study focuses on analyzing the total volume of water retained by the green roof, with emphasis on retention through plant interception in bromeliad tanks and losses due to evapotranspiration. The relevance of these processes to precipitation retention is discussed in order to improve the efficiency of green roofs as a compensatory technique in urban drainage systems and to better understand their hydrological functioning.

Despite the well-documented benefits of green roofs, their implementation also presents relevant limitations that must be acknowledged. Structural constraints of existing buildings may restrict the adoption of green roofs, as not all constructions are designed to support the

additional load imposed by the system layers and retained water [39]. Furthermore, the presence of vegetation capable of storing water, could create favorable conditions for mosquito proliferation if adequate maintenance and drainage are not ensured [40]. Additional challenges include higher installation and maintenance costs, the need for specialized design, and potential operational issues related to waterproofing and long-term performance [41]. Recognizing these constraints is essential for a realistic assessment of green roof applicability in urban environments.

## HYDROLOGICAL CYCLE-PRECIPITATION (INTERCEPTION AND EVAPOTRANSPIRATION)

The hydrological cycle is a global phenomenon of closed circulation of water between the Earth's surface and the atmosphere, driven by solar energy together with the action of gravity and Earth's rotation. The exchange between the circulation of the Earth's surface and the atmosphere occurs in two directions. In the atmosphere-surface sense, where the flow of water occurs in any physical state, the most significant being the precipitation of rain and snow. Through the movement of air masses, the main phenomenon of water transfer from the atmosphere to the surface occurs which is precipitation [42].

When precipitation reaches the ground, part of it infiltrates the soil, part flows over the surface, and part is evaporated, either directly or through the phenomenon known as transpiration [43]. When precipitation falls on soil covered by vegetation, a portion of the precipitated volume is intercepted by leaves and stems, where it is temporarily stored and later evaporates. When the water storage capacity of the vegetation is exceeded, or due to the action of wind, the intercepted water may be re-precipitated onto the soil. Interception is a phenomenon that occurs with both rainfall and snowfall [37].

Interception is the retention of precipitation above the ground surface. Interception may occur through vegetation or other forms of obstruction to runoff. The retained volume returns to the atmosphere through evaporation. This process affects the watershed water balance, as it functions as a reservoir that temporarily stores a portion of the precipitation. The overall tendency of interception is to reduce discharge variability throughout the year, delaying and attenuating flood peaks [44].

According to Tucci and Beltrame [45], interception can be described as the difference between the total precipitation and the portions of the precipitation that cross the vegetation and that drain through the trunk and leaf edges of the trees. The intensity, duration and volume of precipitation influence the interception process, with the largest portion occurring at the beginning of precipitation. Therefore, a rain with a longer duration implies a longer period of time with lower interception rates. Similarly, more intense rains tend to have a smaller portion of the total precipitate being intercepted, since they hinder the retention of water in the foliage and more quickly "saturate" the storage capacity of the vegetation [46].

Of the total precipitation reaching the ground, a portion infiltrates into the soil, another fraction flows as surface runoff, and the remainder returns to the atmosphere through evaporation, either directly from surfaces or indirectly via transpiration [47]. In some regions this evaporation can be so significant that all precipitation is vaporized. At any time or place where water circulates on the Earth's surface, whether on continents or oceans, there is evaporation into the atmosphere, a phenomenon that closes the hydrological cycle. Vegetation characteristics such as leaf density (defined as the number of leaves per unit area and representing the extent of vegetation cover) determine the effective interception area. The size

and shape of the leaves also influences the ability of the vegetation to store water, as well as the arrangement of the trunks, facilitating or not the flow through them [48].

The equations for interception estimation are usually used only for large vegetation, analyzing the portion of precipitation that crosses the vegetation and the portion that flows through the trunks. In this research, due to the size of bromeliads, it is not possible to estimate the interception through these plots. Therefore, in this work an empirical method for the calculation of plant interception will be adopted. Evapotranspiration is the sum of evaporation and transpiration and depends on solar radiation, air vapor stresses and winds [43]. It runs when liquid water is converted to water vapor and transferred to the atmosphere. This process occurs when liquid water is transformed into water vapor and released into the atmosphere. It takes place naturally only when energy is supplied to the system, originating from solar radiation, atmospheric sources, or both, and is governed by the rate of energy transfer associated with the flux of water vapor from the Earth's surface. This transfer occurs in the form of molecular and turbulent diffusion. Therefore, the evapotranspiration process of natural surfaces can be simulated with a physical basis, by models that describe the effect of resistance to molecular and turbulent diffusion on the energy distribution of the sun or atmosphere [37].

Also according to Tucci and Beltrame [45], quantitative information of these processes, which constitute an important phase of the hydrological cycle, are used in solving problems involving water management. However, this information obtained by direct measurements of different locations and different weather conditions is not found in sufficient quantity. Thus, estimates based on physical principles and mainly empirical equations are used as an alternative to fill this gap. Evapotranspiration is considered as the loss of water by evaporation from the soil and transpiration of plants. It is important for the water balance of a basin as a whole. Figure 1 shows the evapotranspiration process.

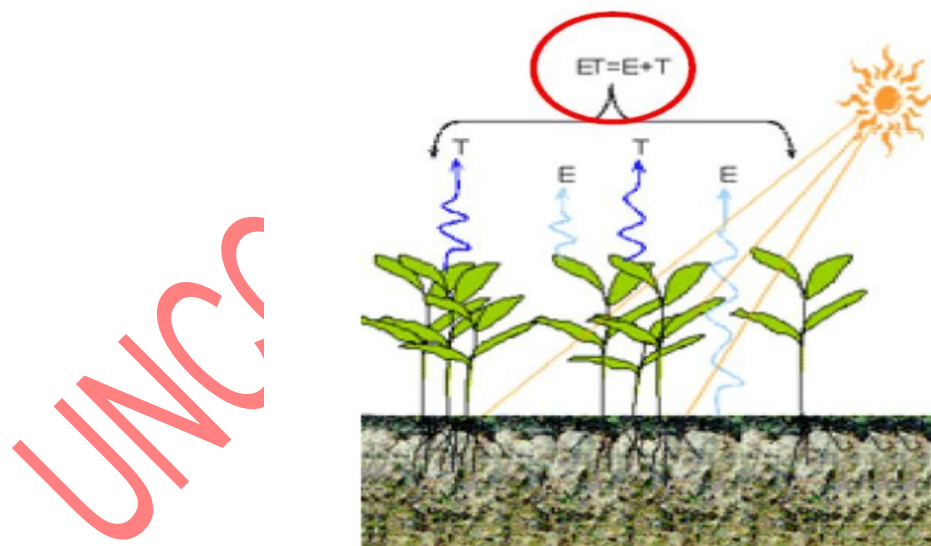


Figure 1 - Representation of evapotranspiration [49]

In the present work, the calculation of the reference evapotranspiration estimate will be made through the Penman-Monteith FAO equation (PM FAO 56), which is an equation that was standardized by the Food and Agriculture Organization of the United Nations (FAO), through the original Penman-Monteith equation. The required data are air temperature, relative humidity, solar radiation and wind speed [50]. The Penman-Monteith FAO equation (PM FAO 56) is found in Equation (1).

$$ET_o = \frac{0,408\Delta(R_n - G) + \gamma \frac{900}{T + 273} u_2 (e_s - e_a)}{\Delta + \gamma(1 + 0,34u_2)} \quad (1)$$

$ET_o$  = reference evapotranspiration (l/d)

$R_n$  = radiation balance at the surface of the culture (MJ m<sup>-2</sup>d<sup>-1</sup>)

$G$  = heat flux density of soil (MJ m<sup>-2</sup>d<sup>-1</sup>)

$T$  = air temperature at 2 m height (°C)

$u_2$  = wind speed at 2 m height (m/s)

$e_s$  = saturation vapor pressure (kPa)

$e_a$  = partial vapor pressure (kPa)

$\Delta$  = slope of saturation vapor pressure curve (°C / °C)

$\gamma$  = psychrometric coefficient (°C / °C)

The assumption of a constant evapotranspiration rate throughout the day was adopted as a modeling simplification due to data availability constraints and the temporal resolution of the measurements. Given the scope of the study and its focus on cumulative water balance and retention performance over daily and longer timescales, short-term diurnal variability in evapotranspiration was considered to have a limited influence on the overall results. This approach is commonly applied in green roof and urban hydrology studies when detailed micrometeorological data are not available, and it provides a reasonable approximation for comparative and exploratory analyses.

## EXPERIMENTAL ANALYSIS

A series of experimental tests was carried out at the Experimental Center for Environmental Sanitation of the Federal University of Rio de Janeiro, where there is a prototype of a green roof composed of bromeliads. To carry out the experimental tests, in addition to the green roof, two other equipment were fundamental: the rain simulator and the rain box. At each test, by sampling, some bromeliads were selected in order to measure the volume of water contained in their tanks. After carrying out the tests, the data obtained are analyzed and, with the help of mathematical and statistical tools, the results obtained are presented in order to have an evaluation of these.

### Description of the prototype of the experiment

The prototype green roof was built at the Experimental Center for Environmental Sanitation (Cesa), located at the Federal University of Rio de Janeiro, University City, in the city of Rio de Janeiro, as shown in Figure 2.



Figure 2 - Location of the Green Roof [51]

The green roof configuration consisted of the following layers: waterproofing layer, draining layer, filtering layer, substrate layer, organic matter layer, substrate protection layer and vegetation layer. The plant layer is composed of bromeliads of the species *Neoregelia Cruenta*, as can be seen in Figure 3. The layers and their thicknesses can be seen in Figure 4.



Figure 3 - green roof bromeliads - species *Neoregelia Cruenta*

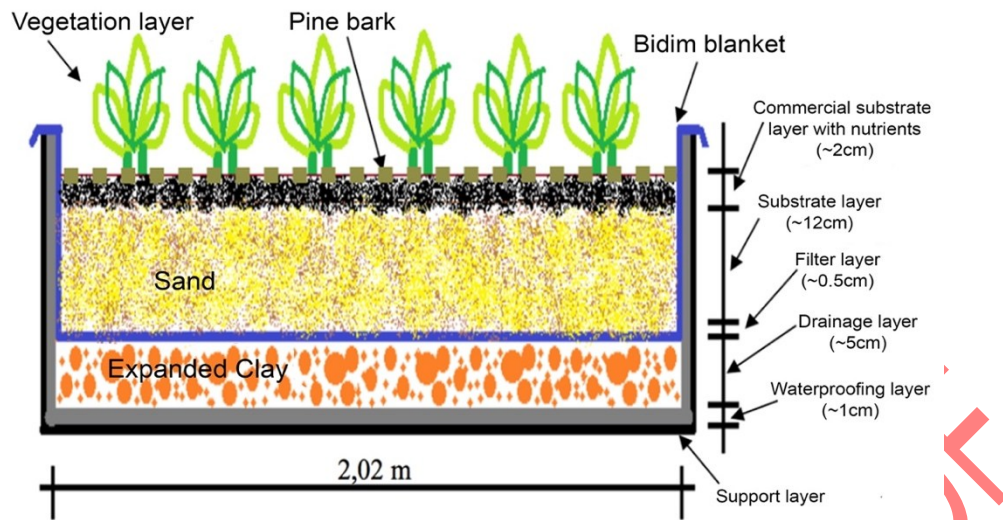


Figure 4 - configuration of green roof layers

Within the volume of water retained by the system, only the volume corresponding to the interception by the bromeliads' vegetation and the volume lost through evapotranspiration will be analyzed. The water retained in the internal layers of the system, such as in the substrate, both at its surface layer and throughout its entire thickness, as well as the volume retained by the drainage layer through the expanded clay will not be analyzed in the present study. Equation (2) represents the components that make up the retained volume.

$$Retained\ Volume = Volume_{Vegetation\ interception} + Volume_{Evapotranspiration} + Volume_{Internal\ layers} \quad (2)$$

The Rain Gauge Box is a device developed by the Polytechnic School of the Federal University of Rio de Janeiro (UFRJ). A patent application for this equipment was filed by the University with the Brazilian National Institute of Industrial Property (INPI) under application number BR2020120286942. The inventor of this device is Professor Theophilo Benedicto Ottoni Filho, from the Department of Water Resources and Environmental Engineering at the Polytechnic School of UFRJ [52].

The equipment was designed to measure the main hydrological processes associated with rainfall, such as total precipitation, infiltration, and surface runoff, as well as to assess the erosion index associated with precipitation events. The Rain Gauge Box is a compact device, built from galvanized steel, with dimensions of 1.00 × 0.90 × 0.70 m, consisting of a main body and a lid [52].

The pluviometer box has three compartments capable of storing water: the pluviometer, the larger reservoir, and the smaller reservoir. Each compartment is connected to a piezometric tube. Piezometric tube 1 is connected to the pluviometer, tube 2 to the smaller reservoir, and tube 3 to the larger reservoir (Figure 5).

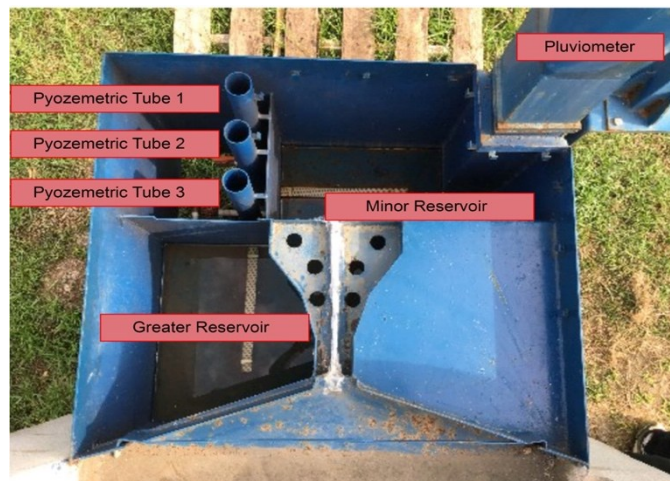


Figure 5 - Rain Gauge box [24]

For the experiments conducted with the green roof, only the larger reservoir, which has an area of 5,400 cm<sup>2</sup>, and piezometer 3, whose tube has an area of 25.52 cm<sup>2</sup>, were used. The reservoir water level is measured manually. A graduated ruler was fixed to the reservoir, and along its entire length a small acrylic tube was glued, through which a metal rod moves. One end of the rod is free, while the other is attached to a small Styrofoam ball that floats according to the water level in the reservoir. The measurement is taken based on a mark on the metal rod. Figure 6 shows the rain gauge box with the installed measuring device, and Figure 7 presents a detailed view of the measuring device.



Figure 6 - Rain Gauge Box and the Level Meter [52]

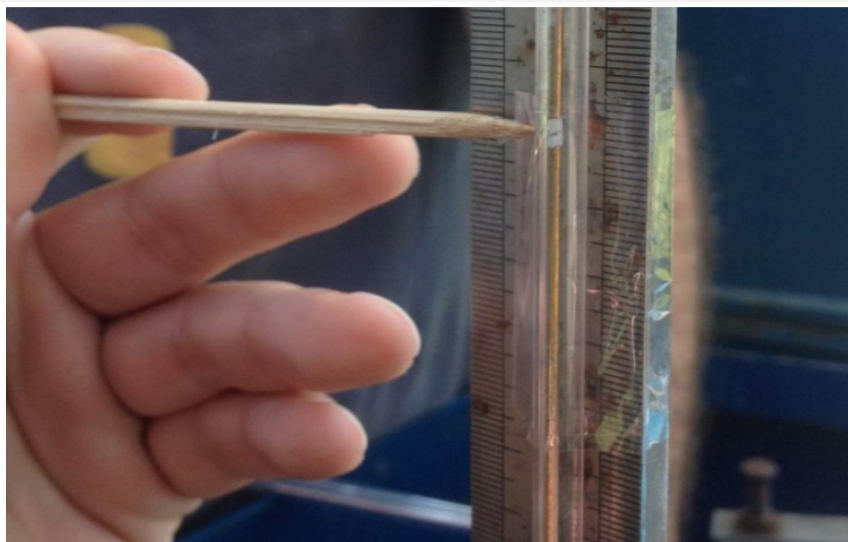


Figure 7 - Detail of the level gauge [52]

The rain simulator consists of a galvanized steel structure with casters at the base, so that it can move on the rails on the experimental bench. In its upper, 2 water interceptors with an adjustable shutter at the bottom, by adjusting the opening of the shutters it is possible to control the intensity of rain. A reservoir with a capacity of 200 liters, two return hoses connecting the interceptors to the reservoir, and a pump. Figure 8 shows the rain simulator.



Figure 8 - Rain simulator [52]

When the system is switched on, the pump conveys water from the reservoir to the water interceptors, which, through the rotation of the shutters, discharge the water through their small openings, thereby simulating rainfall. Excess water returns from the interceptors to the reservoir through return hoses. It is recommended that the water level in the reservoir be kept constant; therefore, throughout the experiment, the reservoir is continuously supplied by a hose connected to the water mains. The pump pressure must also be maintained constant in order to minimize variations in rainfall intensity.

## Experimental method and results

All the tests carried out followed the steps: measurement of the initial volume of water in the bromeliads, measurement of the initial rain intensity (before the test), simulation of the rain on the green roof, measurement of the water drained by the roof in the rain box, measurement of the final rainfall intensity (after the test) and measurement of the final volume of water in the bromeliads.

### Volume of plant interception

Within the volume of water retained by the system, only the volume corresponding to the interception by the bromeliads vegetation and the volume lost through evapotranspiration will be analyzed. The water retained in the internal layers of the system, including the substrate at the surface and throughout its entire depth, is not analyzed in the present study. Similarly, the volume retained by the expanded clay drainage layer, which exhibits retention capacity and is described in detail by Garrido Neto [52], is not considered. Equation (2) represents the components that make up the retained volume.

The initial and final volumes of water inside the bromeliads were measured using a plastic syringe and a graduated Cup. Due to the amount of bromeliads on the roof and the difficulty of removing their water, without the bromeliads being damaged or removed from the ground, the bromeliads that would be analyzed were chosen for each test. This work tried to choose bromeliads of different sizes and characteristics to approximate the global configuration of bromeliads found on the green roof.

Before each test, water was drawn from a syringe by suction and accumulated in the measuring cup until it was no longer possible to draw water from the bromeliad tanks. The volume found was then recorded and the removed water was returned to the interior of the respective Bromeliad. After applying the controlled rain on the roof, a new measurement was made, for the same bromeliads chosen previously, so it was possible to calculate the volume stored by the bromeliad during the test, that is, the plant interception. It should be noted that the measured volumes do not necessarily represent the total storage volume of the bromeliads, since in some cases, small amounts of water were still left in the bromeliads that could not be removed with the syringe, however, due to the fact that a difference in volumes was analyzed, this it does not influence the final result. Still, it is possible that small volume variations were caused by the methodology applied for water withdrawal and the inability of the syringe when trying to withdraw all the water. Figure 9 shows the syringes and measuring cylinder used in the measurement. The syringe used in the measurements had a total capacity of 10 mL with a measurement scale of 1 mL, while the graduated cylinder had a total capacity of 1000 mL with a measurement scale of 10 mL.



Figure 9 - Syringes and measuring cup [52]

### Measurement of Rainfall Intensity

Rainfall intensity is calculated using the following equipment: two metal collecting plates, which together have a total area of 1.8 m<sup>2</sup>, a graduated bucket, and a graduated cylinder. The collecting plates are positioned beneath the rainfall simulator, at the same location where the green roof will be installed. A rainfall event with a duration of 6 minutes is then initiated. After this period, the simulator is turned off and the water accumulated on each plate is transferred to the bucket so that its volume can be measured. For greater accuracy, a graduated cylinder is used.

The volumes of water collected on the two plates are then summed, and rainfall intensity is calculated using Equation (3). This procedure is carried out both before and after the experiment. Due to possible variations in rainfall intensity during the test, the rainfall intensity value adopted is the average of the initial and final rainfall intensities.

$$\text{Rainfall intensity (mm/h)} = \frac{\text{Total water volume (L)}}{\text{Total area of the panels (m}^2\text{)}} + \frac{1}{\text{Rain duration (h)}} \quad (3)$$

With the values already known, the previous equation can be replaced by the Equation (4).

$$\text{Rainfall intensity (mm/h)} = \frac{\text{Total water volume (L)}}{0.18} \quad (4)$$

A Figure 10 illustrates rainfall over the collector plates.



Figure 10 - Simulator and the collector plates [52]

The results of the tests are presented below in Table 1.

Table 1 - Description of tests

Test	Date	Duration (h)	Initial rainfall intensity (mm/h)	Final rainfall intensity (mm/h)	Adopted rainfall intensity (mm/h)
1	20/06/2023	0.5	141.9	153.6	147.8
2	27/06/2023	0.5	136.6	148.3	142.5
3	04/07/2023	0.5	146.1	150.0	148.0
4	11/07/2023	0.5	150.0	134.6	142.3
5	25/07/2023	1.5	97.2	111.8	104.5

### Rainfall simulation and measurement of drained water

After calculating the initial rainfall intensity, the simulator is moved to the green roof to begin the test itself. Once the simulator is in position, the rainfall is initiated and the starting time is recorded. The simulator remains in operation for the predetermined duration of the test. The initial water level inside the rain gauge box must then be recorded.

After some time, the water percolates through the roof layers until it reaches the drains. When the first trickle of water exits the drains and reaches the gutter, the time must be recorded. This corresponds to the elapsed time between the start of rainfall and discharge into the drainage system.

The next step is to record the time required for the water to travel along the entire gutter and drip into the rain gauge box. From that moment on, the water level inside the box is read every 60 seconds and recorded on the field data sheet.

Even after the rainfall ends, measurements must continue and should only stop when the same water level value is observed in five consecutive readings, indicating that the water volume has stabilized and the test has therefore concluded.

The total volume of water precipitated by the simulator can be obtained by multiplying the rainfall intensity, the green roof area (1.78 m<sup>2</sup>), and the rainfall duration, as shown in Equation (5).

$$\text{Precipitated volume (L)} = \text{Rainfall intensity (mm/h)} \times \text{Roof area (m}^2\text{)} \times \text{Rain duration (h)} \quad (5)$$

The volume of water drained into the pluviometer box can be calculated from the variation in the water level inside the box, since the box has known dimensions, as previously stated. Thus, the drained water volume can be expressed by Equation (6).

$$\text{Total accumulated water volume (L)} = \frac{(A_{\text{reserv}} + A_{\text{piezo}}) \times (H_{\text{final}} - H_{\text{initial}})}{1000} \quad (6)$$

Where:

$A_{\text{reserv}}$  = Area of the larger reservoir (5400 cm<sup>2</sup>)

$A_{\text{piezo}}$  = Area of piezometer 3 (25.52 cm<sup>2</sup>)

$H_{\text{final}}$  = Final reading of the water level in the rain gauge box (cm)

$H_{\text{inicial}}$  = Initial reading of the water level in the rain gauge box (cm)

Figure 11 illustrates the drains that convey water from the roof, which, through the gutter, reaches the rain gauge box.



Figure 11 - Green roof and the drains

### Description of the tests

A total of five tests were conducted in June and July 2023, with rainfall starting at approximately 11:00 a.m. The first four tests were performed with a rainfall intensity in the range of 150 mm/h and a duration of 30 minutes. The final test, in order to approximate the conditions used by Garrido Neto (2016), had its intensity adjusted to the range of 100 mm/h and a duration of 1 hour and 30 minutes. The tests are presented below in Table 2.

One factor that directly influences the experimental results is the natural rainfall regime, since the green roof is exposed to weather conditions. To determine the rainfall volume prior to each test, precipitation data from the São Cristóvão Station were obtained from the Alerta Rio platform. Additionally, data from the Rio de Janeiro – Forte de Copacabana Station were collected from the National Institute of Meteorology (INMET) database. The values obtained for the São Cristóvão Station are presented in Table 2, and those for the Forte de Copacabana Station are presented in Table 3.

Table 2 - Data from the São Cristóvão Station

Test	Date	Number of previous days without rain	Cumulative rainfall in the previous 24 h (mm)	Cumulative rainfall in the previous 96 h (mm)
1	20/06/2023	0	4.2	4.2
2	27/06/2023	3	0	4.0
3	04/07/2023	0	0.4	10.6
4	11/07/2023	7	0	0
5	25/07/2023	6	0	0

FONTE: ALERTA RIO [53]

Table 3 - Copacabana Station Data

Test	Date	Number of Previous Days Without Rain	Cumulative Rainfall in the Previous 24 h (mm)	Cumulative Rainfall in the Previous 96 h (mm)
1	20/06/2023	0	6.0	6.0
2	27/06/2023	3	0.0	6.6
3	04/07/2023	0	0.8	22.4
4	11/07/2023	7	0.0	0.0
5	25/07/2023	6	0.0	0.0

FONTE: INMET [54]

## RESULTS OF THE EXPERIMENTAL TESTS

A total of five tests were conducted in June and July 2023, with rainfall beginning around 11:00 a.m. The first four tests were carried out with a rainfall intensity of approximately 150 mm/h and a duration of 30 minutes. The final test, in order to approximate the conditions used by Garrido Neto [28], had its intensity adjusted to approximately 100 mm/h and a duration of 1 hour and 30 minutes. The results of the tests are presented below.

Considering the green roof as a closed system—that is, with no water loss, since the walls and base of the roof are waterproofed, all the water applied by the simulator is either retained within the system or drained into the Rainwater Collection Box (CP). The retained volume is calculated using Equation (7).

$$\text{Retained Volume} = \text{Volume}_{\text{precipitated}} - \text{Volume}_{\text{drained to the CP}} \quad (7)$$

The total volume of water precipitated by the simulator was calculated by multiplying the intensity of rain, the green roof area (1.78 m<sup>2</sup>) and the duration of rain. The volume of water drained into the rain box was calculated by the variation of level inside the box, since the box has known dimensions. The volume of water retained in each of the tests was calculated based on the equations presented previously and are presented in Table 4.

Table 4 - Volume retained in the prototype

Date	Rainfall intensity (mm/h)	Precipitated Volume (l)	Drained Volume for rain gauge box (l)	Retained Volume (l)
20/06/2023	147.8	131.54	26.59	104.95
27/06/2023	142.5	126.83	17.90	108.93
04/07/2023	148.0	131.72	23.87	107.85
11/07/2023	142.3	126.65	22.79	103.86
25/07/2023	104.5	279.02	81.65	197.37

The volume of water intercepted by the roof was calculated from some bromeliads, the characteristics of which are described in Table 5. The volume of water withdrawn before the test is shown in Table 6 and the volume after the test in Table 7. The difference between the two, i.e. the volume actually accumulated during the test is shown in Table 8.

Table 5 - characteristics of bromeliads measured

<b>Characteristics of samples</b>				
<b>Reference</b>	<b>Size</b>	<b>Height (cm)</b>	<b>Leaf Diameter (cm)</b>	<b>Cup diameter (cm)</b>
1	Medium	30	28	4.0
2	Medium	28	27	5.0
3	Small	20	23	4.5
4	Small	14	18	4.0
5	Large	44	39	6.5
6	Large	38	33	5.5
7	Medium	28	33	6.0
8	Large	36	33	7.0
9	Large	35	32	6.0
10	Large	54	30	6.0

Table 6 - Volume of water before the test

<b>Volume before rain (ml)</b>					
<b>Reference</b>	<b>20/06/2023</b>	<b>27/06/2023</b>	<b>04/07/2023</b>	<b>11/07/2023</b>	<b>25/07/2023</b>
1	60	20	45	15	20
2	95	90	150	70	30
3	20	15	15	-	-
4	12	13	12	-	-
5	50	40	-	-	-
6	30	38	-	-	-
7	-	150	130	70	25
8	-	110	75	5	15
9	-	-	70	10	30
10	-	-	-	30	15

Table 7 - Volume of water after the test

<b>Volume after rain (ml)</b>					
<b>Reference</b>	<b>20/06/2023</b>	<b>27/06/2023</b>	<b>04/07/2023</b>	<b>11/07/2023</b>	<b>25/07/2023</b>
1	110	110	100	115	110
2	250	250	265	200	280
3	60	50	55	-	-
4	30	30	30	-	-
5	140	130	-	-	-
6	90	75	-	-	-
7	-	215	230	220	190
8	-	220	250	220	240
9	-	-	110	105	100
10	-	-	-	100	100

Table 8 - Volume of water accumulated during the test

<b>Cumulative Volume (ml)</b>					
<b>Reference</b>	<b>20/06/2023</b>	<b>27/06/2023</b>	<b>04/07/2023</b>	<b>11/07/2023</b>	<b>25/07/2023</b>
1	50	90	55	100	90
2	155	160	115	130	250
3	40	35	40	-	-

<b>4</b>	18	17	18	-	-
<b>5</b>	90	90	-	-	-
<b>6</b>	60	37	-	-	-
<b>7</b>	-	65	100	150	165
<b>8</b>	-	110	175	215	225
<b>9</b>	-	-	40	95	70
<b>10</b>	-	-	-	70	85

To calculate the total volume intercepted by the roof, the *Student's t-distribution* was used to estimate a confidence interval in which lies the average volume of water that each Bromeliad can accumulate. The the *Student's t-distribution* is a continuous probability distribution primarily used in statistical inference when the sample size is small and the population variance is unknown.

For the application of the method, the following parameters are required: number of sample elements (n), sample mean (m), sample standard deviation (s), degree of freedom (v), which is nothing more than the sample size minus one and the choice of confidence level, which in this case was chosen equal to 90%. A 90% confidence level was adopted in the *Student's t-distribution* due to the limited sample size and the exploratory nature of the analysis, aiming to increase the sensitivity for detecting statistically significant differences while maintaining an acceptable level of statistical rigor.

With the values of the confidence level and degree of freedom, through the table *Student's t-distribution* the coefficient is obtained. The confidence interval is described by Equation (8)

$$\left[ m - \frac{s t}{\sqrt{n}}, m + \frac{s t}{\sqrt{n}} \right] \quad (8)$$

Therefore, the average volume intercepted by each Bromeliad will be within the above range, with 90% confidence. To calculate the total intercepted by the entire green roof, simply multiply the values of the interval by the number of bromeliads on the roof (population number =58). The values found for each assay are presented in Table 9.

Table 9 - Volumes of plant interception

Test dates	20/06/2023	27/06/2023	04/07/2023	11/07/2023	25/07/2023
Sample size (n)	6	8	7	6	6
Degrees of freedom (n-1)	5	7	6	5	5
Confidence level	90%	90%	90%	90%	90%
Average (m)	68.83	75.50	77.57	126.67	147.50
Standard Deviation (s)	48.42	46.91	55.19	51.54	77.51
T-student coefficient (t)	2.02	1.89	1.94	2.02	2.02
Lower range	29.00	44.08	37.03	84.27	83.74
Upper range	108.66	109.92	118.11	169.07	211.26

Population numbers	58	58	58	58	58
Minimum volume of population (ml)	168.23	2556.40	2148.01	4887.40	4856.85
Medium volume of population (ml)	3992.33	4379.00	4499.14	7346.67	8555.00
Maximum volume of population (ml)	6302.44	6201.60	6850.28	9805.94	12253.15

The input data required for the Penman-Monteith FAO equation (PM FAO 56), previously presented, were obtained from the National Institute of Meteorology (INMET) database. To improve accuracy, data from two meteorological stations – Rio de Janeiro – Forte de Copacabana and Rio de Janeiro – Vila Militar – were taken, and the reference evapotranspiration value was calculated as the average of both stations. For the purpose of calculation, evapotranspiration is considered to occur on a permanent basis, and its daily value is divided equally over the entire period of one day. Therefore, the evapotranspiration rate corresponding to half an hour will be 48° part of the daily rate, and the volume of evapotranspired water will be calculated by the product of the evapotranspiration rate and the roof area. Table 10 shows the values found.

Table 10 - Evapotranspiration Volume

Test	Duration (h)	Forte de Copacabana Station	Vila Militar Station	Average	Volume of Water (ml)
		ET <sub>o</sub> (mm/d)	ET <sub>o</sub> (mm/d)	ET <sub>o</sub> (mm/d)	
20/06/2023	0.5	1.89	1.82	1.86	68.79
27/06/2023	0.5	2.42	2.14	2.28	84.55
04/07/2023	0.5	2.01	2.04	2.03	75.09
11/07/2023	0.5	2.40	2.28	2.34	86.78
25/07/2023	1.5	2.79	2.65	2.72	302.60

To analyze the contribution of plant interception and evapotranspiration in water retention by the green roof, Table 11 shows the percentages that each volume represents of the total precipitated.

Table 11 - Percentages as a function of precipitated volume

Percentages as a function of precipitated volume						
Test		20/06/2023	27/06/2023	04/07/2023	11/07/2023	25/07/2023
Plant interception volume	Minimum volume	1.28%	2.02%	1.63%	3.86%	2.74%
	Medium volume	3.04%	3.45%	3.42%	5.80%	3.07%

Maximum volume	4.79%	4.89%	5.20%	7.74%	4.39%
<b>Evapotranspiration volume</b>	0.05%	0.07%	0.06%	0.07%	0.11%

From the results of each test, an average percentage value of the volume of plant interception and the volume of evapotranspiration can be obtained, both as a function of the precipitated volume and as a function of the retained volume. These values are shown in Table 12.

Table 12 - Average percentages of volumes retained by interception and evapotranspiration

Average of Tests		Percentage of precipitated volume	Percentage of volume retained
<b>Plant interception volume</b>	Minimum volume	2.31%	2.90%
	Medium volume	3.76%	4.68%
	Maximum volume	5.40%	6.74%
<b>Evapotranspiration volume</b>		0.07%	0.09%

It can be observed that the volume of water found inside the tank of the same Bromeliad, after the rain, practically did not vary from one test to the other, different from the volume found before the rain. This behavior can be attributed to the fact that, after rainfall events, bromeliads tend to be close to their maximum interception capacity. Before rainfall, however, the stored water volume varies according to factors such as air temperature, relative humidity, natural rainfall patterns, initial substrate moisture, and drainage conditions, leading the same bromeliad to exhibit substantially different volumes across experiments.

The value of the contribution of plant interception will be adopted as the mean value of the confidence limit, 3.76% of the precipitated volume and 4.68% of the retained volume. The evapotranspiration volume represents only 0.07% of the precipitated volume and 0.09% of the retained volume. The contribution of plant interception has an important role in the retention of precipitation, being 5.4% and can reach almost 8% of precipitation, if considered the upper limit of the confidence interval presented in table 12.

Through the results obtained it is possible to observe that the contribution of evapotranspiration in retention during a rain event is practically negligible, being only 0.07% of the precipitated volume and reaching a maximum of 0.11% for the last Test. Although evapotranspiration contributes minimally at short temporal scales, its cumulative effect becomes substantial over longer periods, playing a significant role in the overall water balance.

A systematic comparison between the results obtained in this study and those reported in the literature reveals a strong agreement regarding the role of vegetation interception in green roof hydrology. The average interception observed in this study (3.76% of the precipitated volume, reaching up to 5.40% and nearly 8% considering the upper confidence interval) is consistent with values reported by Mendes et al. [37], who found interception capacities on the order of a few millimeters under controlled rainfall conditions, and by Nakayoshi et al. [38], who reported interception values of approximately 6% at the urban scale. This similarity suggests that, despite differences in vegetation type, climatic conditions, and experimental setups, interception tends to represent a relatively small but consistent fraction of total precipitation. In contrast, evapotranspiration showed a negligible contribution at the event scale in the present study (approximately 0.07%), which is also in agreement with previous findings indicating that evaporation losses during short rainfall events are limited, but may become

significant when evaluated over longer temporal scales. Overall, this comparison reinforces the reliability of the experimental approach and highlights that the hydrological behavior observed in bromeliad-based green roofs is coherent with broader patterns reported in the literature.

The greatest contribution to water retention in the green roof comes from its inner layers. It is possible that the main responsible for this is expanded clay, as it is an element that has a high water absorption capacity, around 10% for a period of up to 24 hours according to the CINEXPAN website (<http://www.cinexpan.com.br/>). The green roof prototype turns out to have an internal storage effect, promoted by hydraulic control of the conditions of outflow of the drainage layer, in rains of greater intensity. Thus, water begins to accumulate in the inner layers of the green cover, and can saturate the drainage (expansive clay) and substrate layers (sand and organic soil).

## CONCLUSION

The growth of the global population has intensified urbanization and related problems, such as flooding, which causes significant social, economic, and infrastructural impacts. As a mitigation strategy, green roofs have been proposed as a compensatory urban drainage solution. They reduce peak flows by absorbing and gradually releasing rainfall, while also providing additional benefits such as urban heat island mitigation, noise reduction, and increased biodiversity.

This study presents experimental tests on a green roof prototype and the associated instrumentation. The results show effective stormwater retention, with plant interception within the range reported in the literature. Evapotranspiration values were also consistent with previous studies, although their contribution to short-term retention was relatively low.

The results obtained in this study are consistent with findings reported in the literature, confirming the relevance of vegetation interception in stormwater retention processes. The observed contribution of plant interception, ranging from approximately 5% of the precipitated volume, aligns with results from Mendes *et al.* [22], who reported significant interception under controlled conditions, and Nakayoshi *et al.* [21], who identified interception values around 6% in an urban-scale experiment. Although evapotranspiration presented a negligible contribution in the short term, the findings reinforce that vegetation interception plays an important, albeit secondary, role compared to the storage capacity of the system layers. Overall, the agreement between experimental and bibliographic results supports the reliability of the adopted methodology and highlights the importance of considering both structural and vegetative components in the hydrological performance of green roofs.

The results indicate that more than 90% of the retained water volume is associated not with evapotranspiration or plant interception, but with storage within the internal layers of the system, particularly the substrate and the expanded clay drainage layer. This finding highlights the dominant role of the physical structure of the green roof in stormwater retention and suggests that design parameters related to substrate depth and drainage composition exert a greater influence on water retention performance than vegetation-related processes, especially at short temporal scales.

Future research should expand the analysis of plant interception to different species and further investigate the water retention capacity of green roof layers, such as the expanded clay drainage layer, under natural meteorological conditions. Monitoring both individual rainfall events and longer periods (e.g., weekly or biweekly) would enable evaluation under realistic rainfall variability and provide a more comprehensive understanding of interception,

evapotranspiration, and storage processes. Additionally, future work should include direct comparisons with previously published studies to better contextualize the results, identify trends, and assess system performance under different conditions, thereby strengthening the overall analysis.

## ACKNOWLEDGMENT

The authors would like to acknowledge the support of Conselho Nacional de Desenvolvimento Científico e Tecnológico (CNPq 302618/2026-0), and Fundação Carlos Chagas Filho de Amparo à Pesquisa do Estado do Rio de Janeiro (FAPERJ E-26/210.569/2025 (305234)), and the Grant PID2024-155409OB-C21 funded by MICIU/AEI/10.13039/501100011033/FEDER, EU, which helped in the development of this research.

## REFERENCES

1. A. Vidal, M. K. Najjar, A. N. Haddad, M. Amario, and E. Vazquez, "Permeable Concrete Based on Construction and Demolition Waste Aggregates Used in Permeable Paving Slabs," *J. Sustain. Dev. Energy, Water Environ. Syst.*, vol. 13, no. 2, p. 1130581, 2025, <https://doi.org/10.13044/j.sdewes.d13.0581>.
2. G. Yu, Z. Yu, Z. Chen, and Q. Wang, "Geography and Sustainability Macrosystems ecology: A new engine and frontier in contemporary ecosystem science," *Geogr. Sustain.*, vol. 6, 2025, <https://doi.org/10.1016/j.geosus.2025.100334>.
3. Y. He, C. Lin, C. Wu, N. Pu, and X. Zhang, "The urban hierarchy and agglomeration effects influence the response of NPP to climate change and human activities," *Glob. Ecol. Conserv.*, vol. 51, no. March, p. e02904, 2024, <https://doi.org/10.1016/j.gecco.2024.e02904>.
4. D. G. Angeler, H. B. Fried-petersen, C. R. Allen, S. M. Sundstrom, and C. L. Wonkka, "Adaptive capacity in ecosystems," in *Resilience in Complex Socio-ecological Systems*, 1st ed., vol. 60, Elsevier Ltd., 2019, pp. 1–24.
5. Y. Qian, C. Xia, J. Wang, and J. Tanimoto, "Cross-platform information propagation under environmental feedback with psychological and behavioral control dynamics," *Appl. Math. Comput.*, vol. 523, no. February, p. 130020, 2026, <https://doi.org/10.1016/j.amc.2026.130020> Received.
6. L. Yu and G. Leng, "Global effects of different types of land use and land cover changes on near-surface air temperature," *Agric. For. Meteorol.*, vol. 327, no. August, p. 109232, 2022, <https://doi.org/10.1016/j.agrformet.2022.109232>.
7. S. Santoro, A. Pagano, W. Francesconi, D. Mello, and R. Giordano, "Biodiversity-Climature-Society Nexus assessment through Participatory System Dynamics Model. The case study of Amazon forest-based value chain," *Sci. Total Environ.*, vol. 991, no. June, p. 179893, 2025, <https://doi.org/10.1016/j.scitotenv.2025.179893>.
8. A. Glavina, K. Misic, J. Baleta, J. Wang, and H. Mikulcic, "Economic development and climate change: Achieving a sustainable balance," *Clean. Eng. Technol.*, vol. 26, no. March, p. 100939 Contents, 2025, <https://doi.org/10.1016/j.clet.2025.100939>.
9. P. S. Roy, R. M. Ramachandran, O. Paul, P. K. Thakur, S. Ravan, M. D. Behera, C. Sarangi, and V. P. Kanawade, "Anthropogenic Land Use and Land Cover Changes—A Review on Its Environmental Consequences and Climate Change," *J. Indian Soc. Remote Sens.*, vol. 50, no. 8, pp. 1615–1640, 2022, <https://doi.org/10.1007/s12524-022-01569-w>.
10. S. Wu, L. J. Mickley, J. O. Kaplan, and D. J. Jacob, "Impacts of changes in land use and land cover on atmospheric chemistry and air quality over the 21st century," *Atmos.*

- Chem. Phys.*, vol. 12, no. 3, pp. 1597–1609, 2012, <https://doi.org/10.5194/acp-12-1597-2012>.
11. J. R. Wolch, J. Byrne, and J. P. Newell, “Landscape and Urban Planning Urban green space , public health , and environmental justice : The challenge of making cities ‘ just green enough ,’” *Landsc. Urban Plan.*, vol. 125, pp. 234–244, 2014, <https://doi.org/10.1016/j.landurbplan.2014.01.017>.
  12. P. H. Whitfield, “Floods in future climates: a review,” *Floods Futur. Clim. a Rev.*, vol. 5, pp. 336–365, 2012, <https://doi.org/10.1111/j.1753-318X.2012.01150.x>.
  13. K. P. Dhakal and L. R. Chevalier, “Urban Stormwater Governance: The Need for a Paradigm Shift,” *Environ. Manage.*, vol. 57, pp. 1112–1124, 2016, [Online]. Available: <https://link.springer.com/article/10.1007/s00267-016-0667-5>.
  14. S. M. Rola, L. F. C. Machado, C. Barros-Krause, and L. P. Rosa, “Naturação, água e o futuro das cidades no contexto das mudanças ambientais globais,” in *Congresso Brasileiro de Arquitetos*, 2003, vol. 1, pp. 1–8.
  15. D. Mora-meli, S. L. Carlos, P. Ballesteros-p, and P. Muñoz-velasco, “Viability of Green Roofs as a Flood Mitigation Element in the Central Region of Chile,” *Sustain.*, vol. 2022, pp. 1–19, 2018, <https://doi.org/10.3390/su10041130>.
  16. V. Sousa, M. Carollo, I. Butera, and I. Meireles, “The combined performance of green roof and rainwater harvesting: retention capacity and water saving,” *Blue-Green Syst.*, vol. 7, no. 1, pp. 238–257, 2025, <https://doi.org/10.2166/bgs.2025.041>.
  17. V. Hamouz, P. Møller-pedersen, and T. M. Muthanna, “Modelling runoff reduction through implementation of green and grey roofs in urban catchments using PCSWMM,” *Urban Water J.*, vol. 17, no. 9, pp. 813–826, 2020, <https://doi.org/10.1080/1573062X.2020.1828500>.
  18. M. Giurgiu, I. As, and R. Felseghi, “Assessment of Rainwater Treatment Using Sand and Gravel Filtration and Chlorine Disinfection for Non-Potable Domestic Reuse,” *Buildings*, pp. 1–18, 2025, [Online]. Available: <https://doi.org/10.3390/buildings15203759>.
  19. Z. Dong, D. J. Bain, S. Paudel, J. K. Buck, and C. Ng, “Impact of native vegetation and soil moisture dynamics on evapotranspiration in green roof systems Zhaokai,” *Sci. Total Environ.*, vol. 952, no. August, p. 175747 Contents, 2024, <https://doi.org/10.1016/j.scitotenv.2024.175747>.
  20. L. Locatelli, O. Mark, P. Steen, K. Arnbjerg-nielsen, M. Bergen, and P. John, “Modelling of green roof hydrological performance for urban drainage applications,” *J. Hydrol.*, vol. 519, pp. 3237–3248, 2014, <https://doi.org/10.1016/j.jhydrol.2014.10.030>.
  21. P. Herath, R. Prinsley, B. Croke, J. Vaze, and C. Pollino, “A bibliometric analysis and overview of the effectiveness of Nature-based Solutions in catchment scale flood mitigation,” *Nature-Based Solut.*, vol. 7, no. May, p. 100235, 2025, <https://doi.org/10.1016/j.nbsj.2025.100235>.
  22. G. Baiamonte, “Simplified Interception/Evaporation Model,” *Hydrol. Artic.*, vol. 8, p. 99, 2021, <https://doi.org/10.3390/hydrology8030099>.
  23. D. Dunkerley, “Measuring interception loss and canopy storage in dryland vegetation: a brief review and evaluation of available research strategies,” *Hydrol. Process.*, vol. 14, no. 4, pp. 669–678, Mar. 2000, [https://doi.org/https://doi.org/10.1002/\(SICI\)1099-1085\(200003\)14:4<669::AID-HYP965>3.0.CO;2-I](https://doi.org/https://doi.org/10.1002/(SICI)1099-1085(200003)14:4<669::AID-HYP965>3.0.CO;2-I).
  24. Y. Liu, F. Wang, S. Zhang, W. Ding, R. Li, J. Han, W. Ge, H. Chen, and S. Shi, “Analysis of canopy interception characteristics and influencing factors in typical artificial forest in the Loess Plateau semi-arid region,” *J. Environ. Manage.*, vol. 370, no. 3, p. 122455, 2024, <https://doi.org/10.1016/j.jenvman.2024.122455>.
  25. H. Xu, H. Chen, C. Qian, and J. Li, “The Evapotranspiration Characteristics and Evaporative Cooling Effects of Different Vegetation Types on an Intensive Green Roof:

- Dynamic Performance Under Different Weather Conditions,” *Sustain.*, vol. 16, p. 10812, 2024, <https://doi.org/10.3390/su162410812>.
26. J. Yan, F. Zhang, S. Zhang, W. Liu, S. Zhang, R. Li, Y. He, and K. Wang, “Stormwater retention capacity of blue-green roofs with various configurations: Observational data and modelling,” *J. Hydrol.*, vol. 645, no. PA, p. 132092, 2024, <https://doi.org/10.1016/j.jhydrol.2024.132092>.
  27. N. Prashar, H. Sosan, R. Shaw, and H. Kaur, “Urban Flood Resilience: A comprehensive review of assessment methods, tools, and techniques to manage disaster Naveen,” *Prog. Disaster Sci.*, vol. 20, no. May, p. 100299, 2023, <https://doi.org/10.1016/j.pdisas.2023.100299>.
  28. U. Erdem, A. Sharifi, and Z. Okmen, “Neighborhood-scale assessment of urban flood impacts on transportation network resilience: A case study of Mavis,ehir, İzmir,” *Int. J. Disaster Risk Reduct.*, vol. 132, no. December 2025, 2026, <https://doi.org/10.1016/j.ijdr.2025.105970>.
  29. T. Endendijk, W. J. W. Botzen, H. De Moel, K. Slager, M. Kok, and J. C. J. H. Aerts, “Enhancing resilience: Understanding the impact of flood hazard and vulnerability on business interruption and losses,” *Water Resour. Econ.*, vol. 46, p. 100244, 2024, <https://doi.org/10.1016/j.wre.2024.100244>.
  30. A. Kocornik-mina, T. K. J. Mcdermott, G. Michaels, and F. Rauch, “Flooded Cities,” *Am. Econ. J. Appl. Econ.*, vol. 12, no. 2, pp. 35–66, 2020, [Online]. Available: <https://doi.org/10.1257/app.20170066>.
  31. R. W. Puyt, F. Birger, and C. P. M. Wilderom, “The origins of SWOT analysis,” *Long Range Plann.*, vol. 56, no. 3, p. 102304, 2023, <https://doi.org/10.1016/j.lrp.2023.102304>.
  32. A. Ganthaler, F. Barkmann, G. Leitinger, J. Rüdiger, and S. Mayr, “Living at the edge: Varying substrate depth on green roofs affects the microclimate and plant establishment Andrea,” *Urban For. Urban Green.*, vol. 114, p. 129175, 2025, <https://doi.org/10.1016/j.ufug.2025.129175>.
  33. C. Farrell, X. Q. Ang, and J. P. Rayner, “Water-retention additives increase plant available water in green roof substrates,” *Ecol. Eng.*, vol. 52, pp. 112–118, 2013, <https://doi.org/10.1016/j.ecoleng.2012.12.098>.
  34. C. Szota, C. Farrell, N. S. G. Williams, S. K. Arndt, and T. D. Fletcher, “Science of the Total Environment Drought-avoiding plants with low water use can achieve high rainfall retention without jeopardising survival on green roofs,” *Sci. Total Environ.*, vol. 603–604, pp. 340–351, 2017, <https://doi.org/10.1016/j.scitotenv.2017.06.061>.
  35. A. Kumar, A. Anand, R. V. Singh, R. Kumar, and M. Gohil, “Vegetation hydrology and slope interaction under variable infiltration: a state-of-the-art review,” *J. Infrastruct. Preserv. Resil.*, vol. 6, p. 33, 2025, <https://doi.org/10.1186/s43065-025-00152-0>.
  36. T. Koch, P. Chiffard, P. Aartsma, and K. Panten, “A review of the characteristics of rainfall simulators in soil erosion research studies,” *MethodsX*, vol. 12, no. October 2023, p. 102506, 2024, <https://doi.org/10.1016/j.mex.2023.102506>.
  37. T. A. Mendes, R. D. Alves, G. De Farias, N. Gitirana, S. Pereira, F. Juan, and M. Pereira, “Evaluation of Rainfall Interception by Vegetation Using a Rainfall Simulator,” *Sustain.*, vol. 13, p. 5082, 2021, <https://doi.org/10.3390/su13095082> Academic.
  38. M. Nakayoshi, R. Moriwaki, T. Kawai, and M. Kanda, “Experimental study on rainfall interception over an outdoor urban-scale model,” *Water Resour. Res.*, vol. 45, no. 4, Apr. 2009, <https://doi.org/10.1029/2008WR007069>.
  39. H. Nurdiana, A. Hamid, N. S. Romali, and R. A. Rahman, “Key Barriers and Feasibility of Implementing Green Roofs on Buildings in Malaysia,” *Buildings*, pp. 1–16, 2023, <https://doi.org/10.3390/buildings13092233>.
  40. G. K. L. Wong and C. Y. Jim, “Urban-microclimate effect on vector mosquito

- abundance of tropical green roofs,” *Build. Environ.*, vol. 112, pp. 63–76, 2017, <https://doi.org/10.1016/j.buildenv.2016.11.028>.
41. S. Tabatabaee, A. Mahdiyar, S. Durdyev, and S. Reza, “An assessment model of benefits, opportunities, costs, and risks of green roof installation: A multi criteria decision making approach,” *J. Clean. Prod.*, vol. 238, p. 117956, 2019, <https://doi.org/10.1016/j.jclepro.2019.117956>.
  42. V. Levizzani, “Satellite Remote Sensing of Precipitation and the Terrestrial Water Cycle in a Changing Climate,” *Remote Sens.*, vol. 11, p. 2301, 2019, <https://doi.org/10.3390/rs11192301>.
  43. Nelson L. de Sousa Pinto, A. C. T. Holtz, J. A. Martins, and F. L. S. Gomide, *Hidrologia básica*, 1ª edição. São Paulo, 1976.
  44. J. J. Kurki-fox, B. A. Doll, D. E. Line, M. E. Baldwin, T. M. Klondike, and A. A. Fox, “Estimating Changes in Peak Flow and Associated Reductions in Flooding Resulting from Implementing Natural Infrastructure in the Neuse River Basin, North Carolina, USA,” *Water*, vol. 14, p. 1479, 2022, <https://doi.org/10.3390/w14091479>.
  45. C. E. M. Tucci and L. F. S. Beltrame, *Evaporação e evapotranspiração*, Tucci, C.E. Porto Alegre, 2009.
  46. T. Kim, J. Kim, J. Lee, H. S. Kim, J. Park, and S. Im, “Water Retention Capacity of Leaf Litter According to Field Lysimetry,” *Forests*, vol. 14, p. 478, 2023, <https://doi.org/10.3390/f14030478>.
  47. J. Huang, P. Wu, and X. Zhao, “Catena Effects of rainfall intensity, underlying surface and slope gradient on soil infiltration under simulated rainfall experiments,” *Catena*, vol. 104, pp. 93–102, 2013, <https://doi.org/10.1016/j.catena.2012.10.013>.
  48. P. L. Nagler, E. P. Glenn, T. L. Thompson, and A. Huete, “Leaf area index and normalized difference vegetation index as predictors of canopy characteristics and light interception by riparian species on the Lower Colorado River,” *Agric. For. Meteorol.*, vol. 125, pp. 1–17, 2004, <https://doi.org/10.1016/j.agrformet.2004.03.008>.
  49. UNESP Ilha Solteira, “Importância da Evapotranspiração para a agricultura irrigada,” *ÁREA DE HIDRÁULICA E IRRIGAÇÃO DA UNESP*, 2013. <https://irrigacao.blogspot.com/2013/08/importancia-da-evapotranspiracao-para.html> (accessed Feb. 08, 2026).
  50. L. P. DE ALENCAR, G. C. SEDIYAMA, and E. C. MANTOVANI, “ESTIMATIVA DA EVAPOTRANSPIRAÇÃO DE REFERÊNCIA (ET<sub>o</sub> PADRÃO FAO), PARA MINAS GERAIS, NA AUSÊNCIA DE ALGUNS DADOS CLIMÁTICOS,” *J. Brazilian Assoc. Agric. Eng.*, vol. 4430, pp. 39–50, 2015, <https://doi.org/10.1590/1809-4430-Eng.Agric.v35n1p39-50/2015>.
  51. Google Maps, “centro experimental de saneamento ufrj.” [https://www.google.com/maps/@-22.8618567,-43.2262062,1315m/data=!3m1!1e3?authuser=0&entry=tту&g\\_ep=EgoyMDI2MDIwNC4wIKXMDSoASAFQAw%3D%3D](https://www.google.com/maps/@-22.8618567,-43.2262062,1315m/data=!3m1!1e3?authuser=0&entry=tту&g_ep=EgoyMDI2MDIwNC4wIKXMDSoASAFQAw%3D%3D) (accessed Feb. 08, 2026).
  52. Pedro de Souza Garrido Neto, “TELHADOS VERDES COMO TÉCNICA COMPENSATÓRIA EM DRENAGEM URBANA NA CIDADE DO RIO DE JANEIRO: ESTUDO EXPERIMENTAL E AVALIAÇÃO DE SUA ADOÇÃO NA BACIA DO RIO JOANA A PARTIR DO USO DE MODELAGEM MATEMÁTICA / GREEN ROOFS AS COMPENSATORY TECHNIQUE IN URBAN DRAINAG,” Universidade Federal do Rio de Janeiro, 2016.
  53. Prefeitura do Rio de Janeiro, “Rain forecast today! / Previsão de Chuva HOJE!” <https://alertario.rio.rj.gov.br/> (accessed Feb. 09, 2026).
  54. Ministério da Agricultura e Pecuária, “Análises Meteorológicas / Weather Analysis.” [www.inmet.gov.br/portal/](http://www.inmet.gov.br/portal/) (accessed Feb. 09, 2026).